VEHICLE-TO-GRID BASED FREQUENCY REGULATION METHOD IN AN ISOLATED MICROGRID CONSIDERING CHARGING REQUESTS OF ELECTRIC VEHICLES

Hoyong Jeong
Hyundai Electric & Energy Systems
Korea, Republic of
jeong.hoyong@hyundai-electric.com

Mugu Jeong
Hyundai Electric & Energy Systems
Korea, Republic of
jeong.mugu@hyundai-electric.com

Sangjin Lee
Hyundai Electric & Energy Systems
Korea, Republic of
sangjin.lee@hyundai-electric.com

ABSTRACT

Electric vehicles (EVs) are capable of providing frequency regulation services through Vehicle-To-Grid (V2G). However, EV batteries are different from conventional energy storage systems in the sense that they are originally power load, not only for energy sources. EV owners may require that their charging requests are satisfied while their vehicles even participate in the V2G operation, and therefore, this paper proposed a V2G frequency regulation method in an isolated microgrid considering EV charging requests. The paper presents assumptions necessary for the proposed method and describes a state-of-charge (SOC) management plan and a concept of critical SOC for EV charging requests. In addition, V2G operation scheme for frequency regulation is defined and classified according to the charging requests. Finally, the simulation results using PSCAD/EMTDC and analyses are presented to verifying the effectiveness of the proposed methods.

NOMENCLATURE

$t_{plug\text{-}in}$	Plug-in time of PHEV (hrs)
$t_{plug\text{-}out}$	Plug-out time of PHEV (hrs)
$t_{islanding}$	Time microgrid becomes isolated (hrs)
t_{2nd}	Time secondary reserve is provided (hrs)
t	Current time (hrs)
$T_{primary}$	Duration between $t_{islanding}$ and t_{2nd} (hrs)
T_{remain}	Duration between t_{2nd} and $t_{departure}$ (hrs)
$SOC(t)$	SOC of battery at t (%)
SOC_{crt}	Critical SOC at t_{2nd} (%)
SOC_{req}	Required SOC at plug-out time (%)
SOC_{max}	Maximum SOC of battery (%)
SOC_{min}	Minimum SOC of battery (%)
P_{rated}	Rated power of charger (kW)
P_0	Reference power of charger from aggregator or EMS (kW)
P_{max}	Maximum output power of charger (kW)
P_{min}	Minimum output power of charger (kW)
f_0	Nominal frequency in microgrid (Hz)
$C_{battery}$	Capacity of battery in PHEV (kWh)
η_{charge}	Charging efficiency of EV (%)
$\eta_{discharge}$	Discharging efficiency of EV (%)
DB	Width of dead-band for frequency

INTRODUCTION

Due to the concern about high gas price and global warming, public interest in electric vehicles (EVs) is increasing rapidly. An increase in EVs penetration has a significant impact on power system operation because the vehicles need to be charged, which results in a large amount of electrical energy consumption and affect negatively in terms of power balancing and stability. However, the system operators can utilize EVs as distributed energy resources with vehicle-to-grid (V2G) technology to manage demand and enhance power stability. There have been various studies related to V2G and the detailed concept of V2G has been introduced [1], [2]. V2G can continuously manage load fluctuation and the capability and validation of V2G have been proved [3]. V2G is also suitable for frequency regulation because energy resources are batteries which have fast response characteristic and wide output power range. Many kinds of research have been studied about V2G frequency regulation. The optimal operation of V2G aggregator for frequency regulation was studied [4]. The demonstration results of frequency regulation with V2G and energy storage devices were provided for the PJM systems [5]. The autonomous distributed V2G control and smart charging control scheme were studied for frequency regulation using V2G operation [6]. One of the important issues in the V2G application is charging requests consideration, and it has been dealt with in [7]. More specifically, it proposed a decentralized V2G control scheme to compensate frequency deviation while EV charging requests are satisfied. The previous studies focused on V2G frequency regulation on normal operation condition in a grid-connected power system. However, V2G can be also applied effectively to frequency regulation in a microgrid, especially, operating in island mode. The advantages of V2G operation in an isolated microgrid is described and EVs were utilized as the primary reserve for frequency regulation [8].

During V2G operation, EV batteries might be charged or discharged continuously for frequency regulation in the islanded microgrid. In this situation, desired SOC (state-of-charge) of battery might not be satisfied at time which EV owner want to finish the charging. To address the issue, a new frequency regulation method for V2G operation in an isolated microgrid is proposed with descriptions and assumptions for V2G operation in this paper. More specifically, SOC management plan, the concept of critical SOC and four V2G operation modes in the isolated microgrid are proposed with considering EV charging requests and current battery operating condition. Finally, simulation results illustrate the effectiveness of the proposed methods.

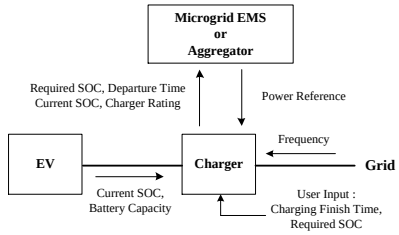

Fig. 1. The signal flows for V2G frequency regulation**.**

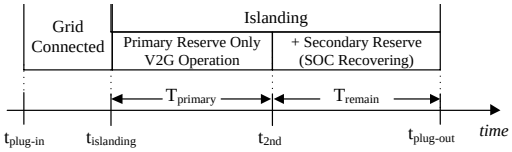

Fig. 2. Operation scheme of the proposed method.

PROPOSED METHOD FOR FREQUENCY REGULATION USING EV

EV Charging Requests and Constraints

EVs could participate in frequency regulation service as distributed energy storage. And EV owners might get an incentive from aggregators or system operators if their vehicles are utilized for V2G operation. Meanwhile, EV owners hope that their vehicle is charged until a certain time they want. It is EV owner's fundamental request, a minimum required SOC at charging-end time and guarantee of the charging completion until the desired time, and these are considered as charging requests in this paper.

Signal Flows for EV Charging and Regulation

Fig. 1 shows signal flows for V2G frequency regulation in the proposed method. Information on battery SOC and capacity is assumed to be obtained by EV chargers. This information works as charging constraints and to determine reference values in the proposed method.

EV users input charging-end time and required SOC information to chargers. EV owners inform their willingness to participate in V2G operation and primary reserve delivery to the aggregator or EMS. Then frequency regulation is activated locally and the corresponding signals are provided by local controllers in each EV charger [10].

Operation Scheme for Microgrid in Islanded Mode

Fig. 2 represents an operation scheme for an isolated microgrid in the proposed method. Loads and generations in the isolated microgrid might not be balanced when there was power flow between main grid and microgrid before disconnection. Frequency is then regulated by primary reserve capacity, and EVs participate in frequency regulation through V2G operation. In the case, EVs should utilize its capacity for frequency regulation as much as possible in the emergency.

It is assumed that sufficient secondary reserve resources are provided to recover frequency at $T_{primary}$ hours after microgrid becomes isolated. Therefore, EV batteries are charged or discharged until secondary reserve resources

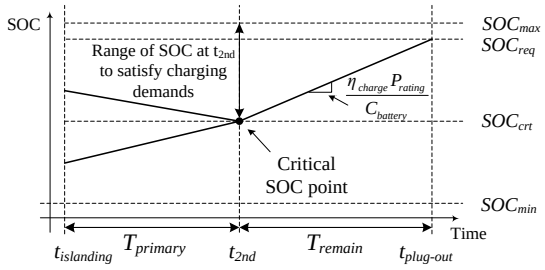

Fig. 3. SOC management plan of the proposed method

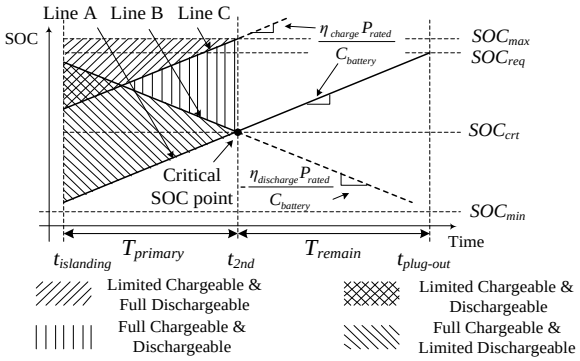

Fig. 4. V2G operation modes defined in proposed method

are provided, and charging plan of each EV is re-scheduled by microgrid EMS or aggregators at t_{2nd} to recover SOC of EV batteries and satisfy charging requests.

SOC Management Plan for V2G Operation

One of the important issues in an isolated microgrid is a SOC management of each EV. EVs should provide its maximum available battery capacity to regulate frequency and, at the same time, charging requests should be also satisfied when EVs are plugged-out. Regarding the requirements, efficient SOC management plan has been established in this paper as explained in Fig. 3.

Minimum battery SOC condition to satisfy the charging condition is presented in Fig. 3 where a solid bold line between $t_{islanding}$ and t_{2nd} indicates a trajectory of SOC when a battery is charged or discharged. Furthermore, a solid bold line between t_{2nd} and $t_{plug\text{-}out}$ presents a trajectory of SOC when SOC of a battery is recovered by charging with the rated power of charger respectively.

Battery SOC should become higher than a minimum required SOC at $t_{plug\text{-}out}$ to satisfy charging requests in Fig. 3. Therefore, each EV should maintain battery SOC above the certain value at t_{2nd} to reach SOC to a minimum required SOC or higher values if battery is charged with its available maximum power after secondary reserve capacity is provided. This certain value is defined as critical SOC point and presented as shown in (1).

$$SOC_{crt} = SOC_{req} - \frac{\eta_{charge} P_{rated}}{C_{battery}} T_{remain} \qquad (1)$$

Definition of V2G Operation Mode

The proposed V2G operation modes are illustrated in Fig. 4. There are three lines between $t_{islanding}$ and t_{2nd}, which are defined as functions of time as shown below.

$$f_A(t) = \frac{\eta_{charge} P_{rated}}{C_{battery}}(t - t_{2nd}) + SOC_{crt} \quad (2)$$

$$f_B(t) = -\frac{\eta_{discharge} P_{rated}}{C_{battery}}(t - t_{2nd}) + SOC_{crt} \quad (3)$$

$$f_C(t) = \frac{\eta_{charge} P_{rated}}{C_{battery}}(t - t_{2nd}) + SOC_{max} \quad (4)$$

Line A in Fig. 4 indicates minimum condition to fulfill charging requests, and battery SOC should be maintained above this condition in a grid-connected mode with considering unexpected grid disconnection. Line B and C indicate a full discharging boundary condition and a full charging boundary condition, respectively. These boundary conditions are important to determine whether the battery could be charged or discharged with maximum power. The EV batteries could be charged or discharged with the rated power of the charger, if the SOC operation point is located below line C or above line B, respectively. However, in the opposite case, maximum allowed charging or discharging power should be limited to maintain battery SOC between maximum SOC and the critical SOC at t_{2nd}.

In this paper, four V2G operation modes during the time between $t_{islanding}$ and t_{2nd} are defined with considering a minimum condition to fulfill charging requests, a full charging boundary condition, and a full discharging boundary condition.

The V2G operation mode is defined as 'limited chargeable and full dischargeable mode' if the SOC operation point is located above the lines B and C. In the mode, the EVs could discharge their batteries with the rated power of charger. But charging power is limited because battery SOC is too high to be charged with a large amount of power. A maximum chargeable power, which equals a minimum dischargeable power, is set to be the value that results in the maximum battery SOC at t_{2nd} if the battery is charged with the maximum chargeable power during the time period between t and t_{2nd}. The maximum and minimum dischargeable power of charger and the SOC condition for the mode are presented as (5)-(7), respectively. The positive and negative values mean that the battery is being discharged or charged.

$$P_{max} = P_{rated} \quad (5)$$

$$P_{min} = \frac{C_{battery}\left[SOC(t) - SOC_{max}\right]}{\eta_{charge}(t_{2nd} - t)} \quad (6)$$

$$SOC(t) \geq f_B(t) \ \ and \ \ SOC(t) \geq f_C(t) \quad (7)$$

If the SOC operation point is located below line B and above line C, the V2G operation mode is defined as 'limited chargeable and dischargeable mode'. The charging and discharging power in this mode could not be the rated power of charger due to SOC constraints at t_{2nd}. Instead in the case, maximum dischargeable power is set to be the value causing the SOC to be reached the critical SOC point if the battery is discharged with maximum dischargeable power during the time period between t and t_{2nd}. The minimum dischargeable power is also determined from (6). The maximum and minimum power and SOC conditions for this mode are expressed as follows:

$$P_{max} = \frac{C_{battery}\left[SOC(t) - SOC_{crt}\right]}{\eta_{discharge}(t_{2nd} - t)} \quad (8)$$

$$f_C(t) \leq SOC(t) \leq f_B(t) \quad (9)$$

The other modes, 'full chargeable and dischargeable mode' and 'full chargeable and limited dischargeable mode', are also defined similarly with modes explained above, and the only difference is a minimum power when battery could be charged with the rated power of charger, as represented in (10).

$$P_{min} = -P_{rated} \quad (10)$$

Finally, the four V2G operation modes are summarized as Table 1.

SIMULATIONS AND RESULTS

Test System and Simulation Scenarios

Fig. 5 shows a single-line diagram of the 22.9kV microgrid test system connected to the main grid system, which base voltage is 154 kV and nominal frequency is 60 Hz, through the static switch. The test system is constructed based on the IEEE 13-bus distribution system and it is assumed that the system is 3 phase-balanced. There are constant power loads which capacity is 2 + j0.66 MVA. Two inverters based distribution generators (DGs), which rated power is 1.4 MVA and 1.2 MVA, is connected and reference power is 0.8 MW and 0.95 MW, respectively. Droop constants of DGs are 3 Hz/MW and 4 Hz/MW respectively. $T_{primary}$ is 1/6 hours and the allowed frequency deviation of the system is 0.1 Hz. The 10 groups of EVs are connected and

Table 1. SOC Condition, maximum and minimum power of each V2G operation mode

No	V2G operation Mode	Maximum power	Minimum Power	SOC condition for mode
1	Limited chargeable and full dischargeable mode	P_{ratied}	$\frac{C_{battery}\left[SOC(t) - SOC_{max}\right]}{\eta_{charge}(t_{2nd} - t)}$	$SOC(t) \geq f_B(t)$ and $SOC(t) \geq f_C(t)$
2	Limited chargeable and dischargeable mode	$\frac{C_{battery}\left[SOC(t) - SOC_{crt}\right]}{\eta_{discharge}(t_{2nd} - t)}$	$\frac{C_{battery}\left[SOC(t) - SOC_{max}\right]}{\eta_{charge}(t_{2nd} - t)}$	$f_C(t) \leq SOC(t) \leq f_B(t)$
3	Full chargeable and dischargeable mode	P_{rated}	$-P_{rated}$	$f_B(t) \leq SOC(t) \leq f_C(t)$
4	Full chargeable and limited dischargeable mode	$\frac{C_{battery}\left[SOC(t) - SOC_{crt}\right]}{\eta_{discharge}(t_{2nd} - t)}$	$-P_{rated}$	$SOC(t) \leq f_B(t)$ and $SOC(t) \leq f_C(t)$

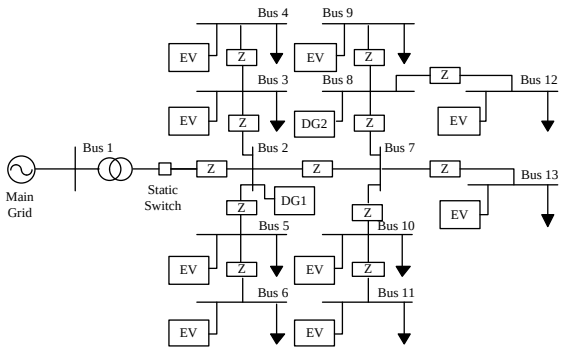

Fig. 5. Single-line diagram of the microgrid test system

Table 2. Parameters of EVs in the microgrid test system

Group No.	Bus No.	$t_{plug\text{-}out}$ (+hrs)	$SOC_{required}$ (%)	SOC at $t_{islanding}$ (%)	$C_{battery}$ (kWh)	P_0 (kW)
1	3	0.3	90	80	5	-3
2	4	2	80	40	15	-3.5
3	5	1.5	85	40	15	-1
4	6	5	90	75	5	0
5	8	0.5	85	70	15	-2
6	9	3	85	60	20	0
7	10	3.5	90	40	5	-1
8	11	4	90	30	20	-2
9	12	1.5	90	85	5	-3
10	13	2	85	40	20	-2.5

each group has 5 EVs. EVs in the same group have identical charging conditions, which is shown in Table 2. The maximum and minimum SOC of all EVs are 0.95 and 0.15, respectively. The rated power of all of the EV charger is 5 kW and it is assumed that the charging and discharging efficiency are both 0.95. Whole components of the test system are modeled using the PSCAD/EMTDC.

The simulation sequence is as follows: the system operates in a grid-connected mode initially and it is disconnected from the main grid at 0.1 sec. The EVs then participate in the V2G frequency regulation. The SOC of each EV group is observed to verify whether the charging requests are satisfied. Two simulation cases are considered for V2G frequency regulation with considering the microgrid in an islanded-mode as follows:

Case 1: EV charging requests are not considered. Frequency is regulated by droop control. Droop constant of all EVs is 0.25 Hz/kW.

Case 2: EV Charging requests are considered. Frequency is regulated by droop control. Droop constant of all EVs is 0.25 Hz/kW.

Results of Case 1

The grid frequency and output power of DGs and EVs for case 1 are presented in Fig. 6(a) and (b). After the microgrid was disconnected from the main grid, the frequency was maintained at 59.329 Hz it was increased to 59.349 Hz at 366.3s because EV battery SOC became full and charging power became zero in group 9.

The results of case 1 present charging requests of some vehicles could not be satisfied. In Table 3 and Fig. 7, the SOC at t_{2nd} of EV group 3 and 5 was lower than critical SOC, and it means their battery SOC could not be reached to the required SOC although EV is charged to maximum chargeable power after the secondary reserve is provided.

Table. 3. The simulation results of case 1

Group No.	SOC at $t_{islanding}$ (%)	SOC at t_{2nd} (%)	$SOC_{critical}$ (%)	Charging request satisfaction
1	80	88.23	77.33	O
2	40	43.30	21.94	O
3	40	40.52	42.78	X
4	75	73.23	≤ 0	O
5	70	71.63	74.44	X
6	60	59.56	17.71	O
7	40	41.56	≤ 0	O
8	30	31.22	≤ 0	O
9	85	90.00	≤ 0	O
10	40	41.64	41.46	O

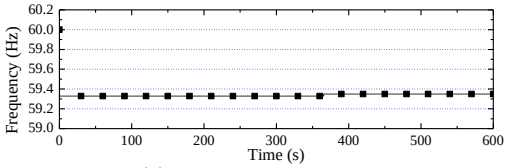

(a) Frequency response

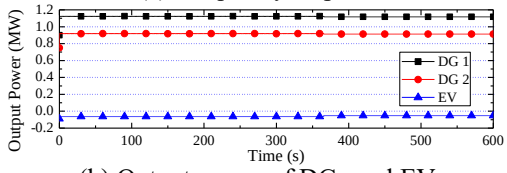

(b) Output power of DGs and EVs

Fig. 6. The simulation results for case 1

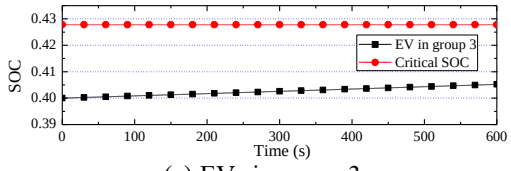

(a) EVs in group 3

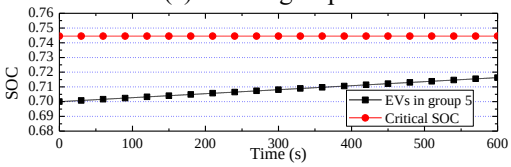

(b) EVs in group 5

Fig. 7. SOC variation and critical SOC for case 1

This is because droop constant and discharge power are determined without consideration of charging requests for frequency regulation.

Results of Case 2

The simulation results of case 2 are presented in Fig. 8 and Table 4 and the V2G operation mode in Table 4 indicates the mode in Table 1. The frequency was 59.297 Hz, which is 0.052 Hz lower than the case 1, after isolation of the microgrid. This is because maximum dischargeable power of some vehicles, whose V2G operation mode is 2 or 4, was limited by the proposed method. However, the frequency was increased gradually and it reached to 59.330 Hz at t_{2nd} because maximum dischargeable power of some vehicle increasing between $t_{islanding}$ and t_{2nd}.

Table 4 summarizes that the SOC at t_{2nd} of all EVs is equal to or higher than the critical SOC and Fig. 9 shows SOC of EVs in group 3 and 5 reached to critical SOC at t_{2nd} contrary to the case 1. It implies that the charging requests

Table. 4. The simulation results of of case 2

Group No.	SOC at $t_{islanding}$ (%)	SOC at t_{2nd} (%)	$SOC_{critical}$ (%)	Charging request satisfaction	V2G operation mode
1	80	88.06	77.33	O	2 to 1 at 330.9s 1 to 3 at 450.0s
2	40	43.24	21.94	O	3
3	40	42.78	42.78	O	4
4	75	73.06	≤ 0	O	1 to 3 at 29.1s
5	70	74.44	74.44	O	4
6	60	59.51	17.71	O	3
7	40	41.39	≤ 0	O	3
8	30	31.18	≤ 0	O	3
9	85	90.00	≤ 0	O	1
10	40	41.60	41.46	O	4 to 3 585.1s

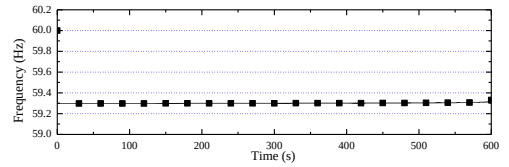

(a) Frequency response

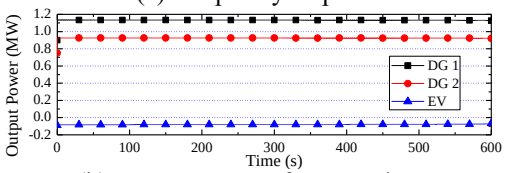

(b) Output power of DGs and EVs

Fig. 8. The simulation results of case 2

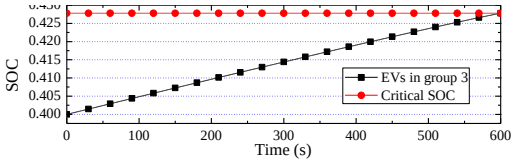

(a) EVs in group 3

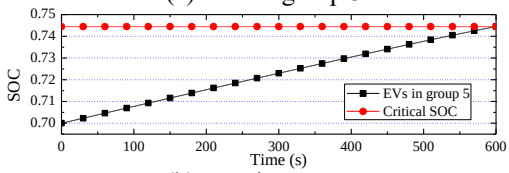

(b) EVs in group 5

Fig. 9. SOC variation and critical SOC of case 2

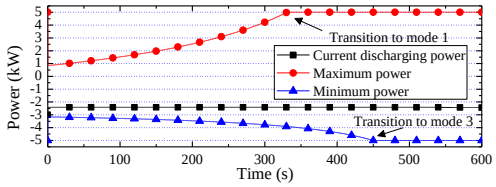

Fig. 10. Power limit of EVs in group 1 of case 2

of all EVs are fulfilled by the proposed method. Fig. 10 presents the maximum and minimum power of EVs in group 1 is changed during V2G operation and power was limited by the proposed method continuously to satisfy the charging requests. Initially, the EV group 1 participates in the V2G operation with mode 2 after the microgrid is isolated. And then, The V2G operation mode was changed to mode 1 at 330.9s because the maximum dischargeable power reaches the rated power of a charger. At 450.0s, the V2G operation mode is changed to mode 3 and minimum dischargeable power becomes the negative value of rated power of charger. It represents that V2G operation modes could be changed continuously and limit charging or discharging power according to charging condition and frequency of the microgrid.

CONCLUSION

This paper proposed a new V2G frequency regulation method considering the EV charging requests in the isolated microgrid. The SOC management plan for V2G operation and the concept of the critical SOC are described in detail. They represent the condition and the criteria of the charging request satisfaction respectively. Based on the SOC management plan and critical SOC rule, the proposed V2G operation modes guaranteed the charging requests of each EV. The simulation results proved the effectiveness of the proposed method, presenting that all EVs are satisfying charging requests. A transition of V2G operation modes also indicates that proposed methods are working properly when the charging conditions and operation conditions of microgrid change continuously.

REFERENCES

[1] Lund, Henrik and W. Kempton, 2008, "Integration of renewable energy into the transport and electricity sectors through V2G," *Energy Policy*, vol.36, no.9, pp.3578-3587.

[2] W. Kempton, Willett, 2005, Tomie and Jasna, "Vehicle-to-grid power fundamentals: Calculating capacity and net revenue", *Journal of Power Sources*, vol.144, no.1, pp.268-279.

[3] B. Kramer, S. Chakraborty and B. Kroposki, 2008, "A review of plug-in vehicles and vehicle-to-grid capability," *Industrial Electronics, 2008. IECON 2008. 34th Annual Conference of IEEE*, Orlando, United States.

[4] S. Han, S Han, and K. Sezaki, 2010, "Development of an optimal vehicle-to-grid aggregator for frequency regulation," *IEEE Transactions on Smart Grid*, vol.1, no.1, pp.65-72.

[5] W. Kempton, V. Udo, K. Huber, K. Komara, S. Letendre, S. Baker, D. Brunner, and N. Pearre, 2008, *A Test of Vehicle-to-Grid (V2G) for Energy Storage and Frequency Regulation in the PJM System*, Univ. of Delaware

[6] Y. Ota, H. Taniguchi, T. Nakajima, K. M. Liyanage, Jumpei Baba, and A. Yokoyama, 2012, "Autonomous Distributed V2G (Vehicle-to-Grid) Satisfying Scheduled Charging," *IEEE Transactions on Smart Grid*, vol.3, no.1, pp.559-564.

[7] H. Liu, Z. Hu, Y. Song and J. Lin, 2013, "Decentralized Vehicle-to-Grid Control for Primary Frequency Regulation Considering Charging Demands," *IEEE Transactions on Power System,* vol.28, no.2, pp.1-10.

[8] Lopes J.A.P., Soares F.J., and Almeida P.M.R., 2011, "Integration of Electric Vehicles in the Electric Power System," *Proceedings of the IEEE*, vol.99, no.1, pp.168-183.